Electronic fluctuation in physiological solutions: Trimethylamine *N*-oxide and *tert*-butyl alcohol

Nahoko Kuroki[1,2], Yukina Uchino[3], Tamon Funakura[1], and Hirotoshi Mori[1,4]**

[1]Department of Applied Chemistry, Faculty of Science and Engineering, Chuo University; Bunkyo-ku, Tokyo, 112-8551, Japan.

[2]JST, ACT-X; Kawaguchi, Saitama, 332-0012, Japan.

[3]Department of Chemistry and Biochemistry, Graduate School of Humanities and Sciences, Ochanomizu University; Bunkyo-ku, Tokyo, 112-8610, Japan.

[4]Department of Theoretical and Computational Molecular Science, Institute for Molecular Science; Myodaiji, Okazaki, 444-8585, Japan.

*To whom correspondence may be addressed.

Email: kuroki.91d@g.chuo-u.ac.jp, qc-forest.19d@g.chuo-u.ac.jp

ABSTRACT

Although small organic molecules in cells have been considered important to control the functions of proteins, their electronic fluctuation under real physiological conditions has never been clarified due to the lack of observations. Herein, the time evolutions of the interactions in dilute aqueous trimethylamine *N*-oxide (TMAO) and *tert*-butyl alcohol (TBA) solutions were analyzed via *ab initio* molecular dynamics simulations accelerated with the fragment molecular theory. It has been known that TMAO and TBA have similar structures, but opposite physiological functions to stabilize and destabilize proteins. It was clarified that water dipole in the TMAO solutions are up to 1.5 times enhanced that affect protein stabilization. Understanding the solution dynamics will contribute to artificial chaperone design in next generation medicine.

1. INTRODUCTION

Small organic solutes in cells have various effects on proteins. For example, trimethylamine *N*-oxide (TMAO, Figure S1a), which consists of N^+O^- and methyl (CH_3–) groups, has been found in deep-sea fishes and is a known osmolyte that preserves the physiological functions of proteins.[1] However, the preservation mechanism of the osmotic pressure is still under debate; the proposed explanations include an attractive direct interaction between TMAO and proteins[2] or indirect interactions *via* structural changes of an aqueous solution as a molecular aggregate.[3,4] If the mechanism by which TMAO allows physiological functional preservation in proteins is clarified, it would make fundamental scientific contributions to, for example, the next generation of medicine by accelerating the development of artificial chaperones and understanding the mechanism of atherosclerosis. Therefore, it is necessary to understand the fundamental physical properties of TMAO.

The biophysical chemistry and solution dynamics of aqueous TMAO solutions have been extensively investigated from experimental[5–14] viewpoints. Vibrational and nuclear magnetic resonance spectroscopy indicated that both the N^+O^- and CH_3– groups of TMAO slow the dynamics of water molecules in a solution and that the N^+O^- groups have a notable ability to capture water molecules.[5–7, 10, 11, 13] *Ab initio* molecular dynamics (AIMD) simulations are essential for explaining the experimental results precisely, because of the fluctuating polarization interactions in the aggregated systems. Although there have been several sub-picosecond-order AIMD simulations,[15–20] there have been no nanosecond-order AIMD simulations while reproducing the TMAO concentration and diffusion coefficients of water in deep-sea fishes. Additionally, it has been impossible to trace the complex intermolecular interaction networks in the hydrated systems at molecular level back to their origin.

To track the time evolution of intermolecular interactions with high accuracy, we applied the AIMD methods based on the fragment molecular orbital and effective fragment potential (EFP) methods.[21–25] The EFP method is particularly suited to performing nanosecond-order AIMD simulations for systems containing several thousand atoms; it has been applied to clarify thermodynamic properties under varying conditions of pressure, temperature, and concentration, due to its high accuracy and efficiency.[23–25] In this research, a set of *ab initio* EFP-MD simulations (2.5 ns for production) was conducted on dilute aqueous TMAO solutions (0.18 mmol L^{-1}) to clarify the effect of the TMAO solute on the dynamics of the system. For comparison, a dilute aqueous solution of *tert*-butyl alcohol (TBA, Figure S1b) was investigated. Both TMAO and TBA are amphiphilic solutes. Herein, unlike TMAO, TBA is known as a protein denaturant.[5, 6, 26]

2. COMPUTATIONAL METHOD

The structures of TMAO, TBA, and H_2O molecules in the gas phase were optimized using the Gaussian16 quantum chemistry program package.[27] The MP2/aug-cc-pVTZ[28] level of theory was applied to the calculations, and the natural bond orbital (NBO) analysis was performed. The T_1 diagnostic values[29] of TMAO, TBA, and H_2O molecules were 0.013, 0.010, and 0.010, respectively, confirming that there was no multireference nature. Using the wavefunctions for the optimized molecules, the EFPs were defined by the "MAKEFP" module implemented in the GAMESS-US program package.[30]

Before performing the EFP-MD simulations, we evaluated the accuracy of the EFPs. For this purpose, we decomposed the total interaction energies obtained by the quantum chemistry

calculations (MP2/aug-cc-pVTZ) into E^{ES}, E^{EXREP}, $E^{POL}+E^{CT}$, and E^{DISP} through LMO-EDA[31] and compared them with the EFP results. In the LMO-EDA calculations, we applied the counterpoise method to correct the basis set superposition errors. Subsequently, we performed a set of EFP-MD simulations for dilute TMAO or TBA aqueous solutions and pure water. In the EFP-MD simulations, we used a set of cubic periodic boxes with a side length of ~21 Å containing one solute molecule and 300 H_2O molecules with a canonical (NVT) ensemble and a cutoff distance of 10 Å. The simulation box size was defined to model the dilute aqueous solution (0.18 mmol L^{-1}). In the EFP-MD simulations, we used a time step of 1 fs and a temperature of 298.15 K (defined using a Nosé–Hoover thermostat). Under these conditions, a set of at least 0.8 ns equilibration and 2.5 ns production runs were performed to evaluate the self-diffusion constants, hydrogen-bond dynamics, radial distribution functions (RDFs), and time-dependent intermolecular interaction energies.

3. RESULTS AND DISCUSSION

The chemical accuracy of EFPs was verified for TMAO, TBA, and H_2O. The EFPs reproduced dipole moments via high-precision *ab initio* quantum chemical calculations within a 0.14 D error, which is more accurate than that of classical force field models[26, 32] (Table S1). The structural parameters of TMAO/TBA–H_2O dimer models optimized by the EFPs agreed with the MP2 level of quantum chemistry calculation results within 0.14 Å (Figures S2, S3, and Tables S2, S3). The slight difference in dimer formation validates the rigid rotor approximation in the EFP method, at least within our target systems. The total interaction energy and its components, calculated by the EFP method, near the stable conformation of the TMAO/TBA–H_2O dimer,

accurately reproduced the corresponding localized molecular orbital energy decomposition analysis (LMO-EDA)[31] at the MP2 level (Figures S4, S5). The mean absolute error (MAE) of the total interaction energy obtained by EFP and MP2 was 1.3 kcal mol^{-1}. The MAE of each interaction energy component (electrostatic (E^{ES}), exchange-repulsion (E^{EXREP}), polarization (E^{POL}) with charge-transfer (E^{CT}), and dispersion (E^{DISP})) was 0.7, 0.6, 1.4, and 0.5 kcal mol^{-1}, respectively. The H_2O–H_2O interaction described by the EFP method has been established previously.[24] The chemical accuracy of the EFP method was thus confirmed.

One of the ways for validating the MD simulations is by comparing theoretically predicted transport properties with experimental results. Herein, the self-diffusion coefficients were calculated using Einstein's equation (Eq. 1).

$$D = \lim_{t\to\infty} \frac{1}{6t} \langle |\boldsymbol{r}_i(t) - \boldsymbol{r}_i(0)|^2 \rangle \qquad (1)$$

The diffusion coefficient of water (D_{water}) was experimentally observed to be 2.3×10^{-9} m^2 s^{-1},[33] while our simulations provided a value of 2.4×10^{-9} m^2 s^{-1} (Table S4). It has been experimentally observed that D_{water} in a dilute aqueous TMAO solution (~0.2 mmol L^{-1}) is ~10% lower than that in pure water.[34] Thus, our nanosecond-order *ab initio* EFP-MD results successfully reproduced that TMAO slows the dynamics of water molecules.

Several solute–solvent site radial distribution functions (RDFs) were calculated to investigate dilute aqueous TMAO/TBA solutions (Figure 1 and Table S5). The coordination numbers of the top sites of solutes were evaluated by integrating the RDFs for $O_{TMAO/TBA}$–O_{water} and $O_{TMAO/TBA}$–H_{water} for the range up to the first minima. The coordination number calculated using $O_{TMAO/TBA}$–O_{water} was 3.3 for both TMAO and TBA, while those calculated using $O_{TMAO/TBA}$–

H_{water} were 3.3, and 2.0 for TMAO and TBA, respectively. These results indicate that the hydrophilic groups of TMAO firmly trap three H_2O molecules as hydrogen-bond donors, while those of TBA coordinate two H_2O molecules and one H_2O molecule as hydrogen-bond donors and acceptors, respectively. Focusing on the bottom sites of TMAO and TBA, that is, the coordination numbers of $X_{TMAO/TBA}$–O_{water}, it is apparent that the CH_3– groups of TMAO and TBA have different hydration properties. Therefore, the RDFs for X_{TBA}–O_{water} have no peaks within 2 Å, while X_{TMAO}–O_{water} has a coordination number of 0.7. The CH_3– groups of TBA exhibit "hydrophobic hydration," while those of TMAO proactively trap H_2O molecules. The CH_3– groups of TMAO and TBA enact differently in dilute solutions.[5, 35]

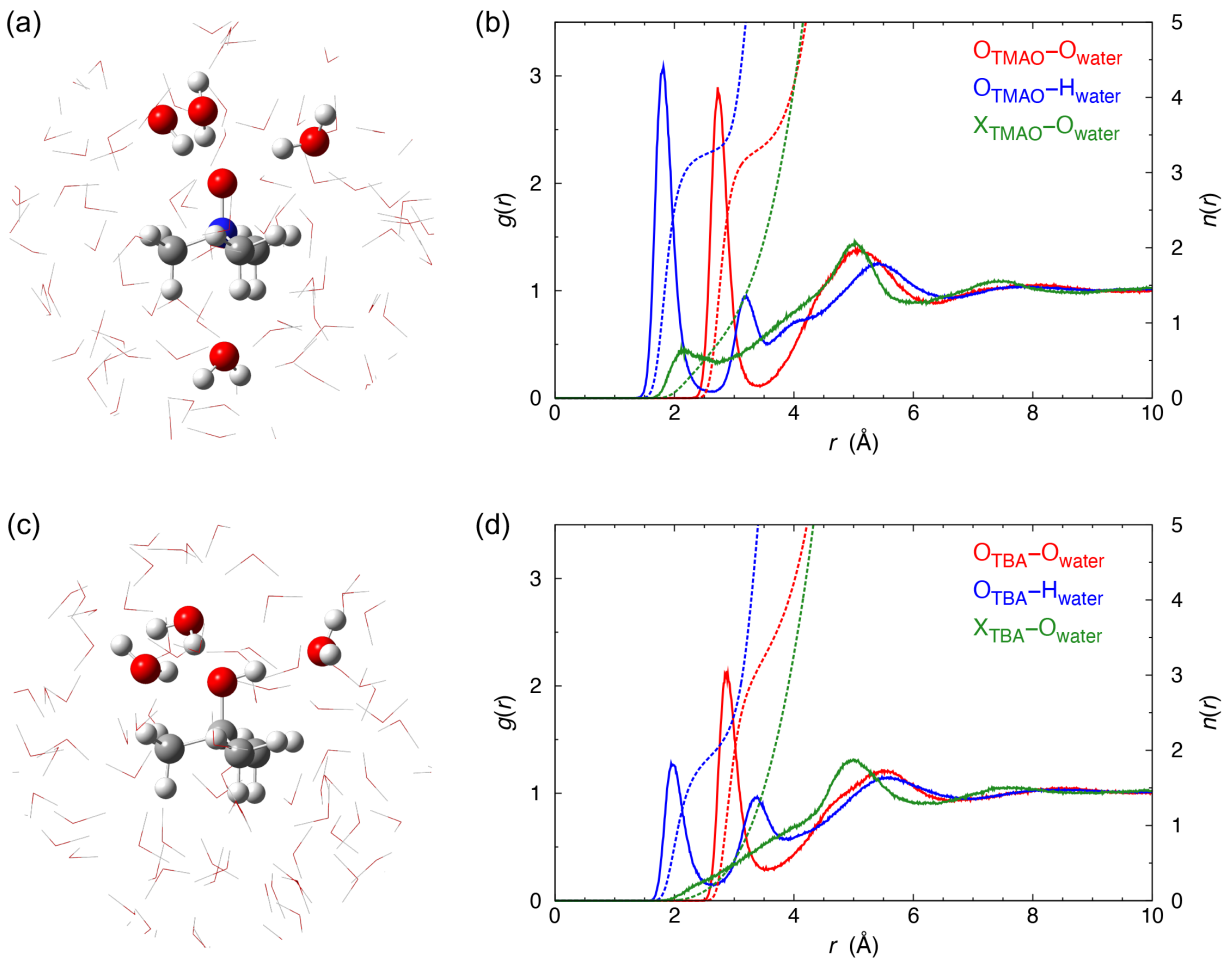

Figure 1. Solution structures simulated by EFP-MD. (a) Snapshot of aqueous TMAO. (b) Solute–solvent site RDFs, g(r), and hydration numbers, n(r), for aqueous TMAO. (c) Snapshot of aqueous TBA. (d) Solute–solvent site, g(r) and n(r), for aqueous TBA. XTMAO/TBA was defined as the center of mass of the three axial hydrogen atoms of the CH3– groups in TMAO/TBA.

The hydrogen-bond correlation function ($p_{HB}(t)$)[36] (Eq. 2) was calculated to clarify the effect of the N^+O^-, OH, and CH_3– groups of each solute on the kinetics of the water molecules in the dilute aqueous TMAO/TBA solutions (Figure S6).

$$p_{HB}(t) = \frac{\langle h(0)h(t)\rangle}{\langle h(0)\rangle} \quad (2)$$

Here, the hydrogen-bond formation function ($h(t)$) is a step function defined as 1 when the distance between each solute and solvent site is smaller than the first minimum of each RDF (Table S5). Otherwise, $h(t)$ is defined as 0. The TMAO/TBA···H_2O hydrogen-bond lifetimes (Table S6) were evaluated by fitting $p_{HB}(t)$ to $ae^{-t/\tau_a} + be^{-t/\tau_b}(a + b = 1)$ to the data in the range $0.0 < t < 100$ ps (Figure S6); the double exponential fitting was applied since it provided better results than those from the single exponential fitting.

The EFP-MD results indicated that the N^+O^- group of TMAO and the OH group of TBA captured three H_2O molecules with an average lifetime of 31.2 and 16.5 ps, respectively. The calculated lifetime for TMAO agreed with those obtained by dielectric spectroscopy (at least 50 ps at ~300 K)[13] and previous AIMD simulations (30–50 ps at 320 K; for D_2O solution)[15]. The hydrogen-bond lifetime near the CH_3– group of TBA was 0.1 ps, while that near TMAO was significantly longer, 6.9 ps. It was confirmed that the CH_3– groups of TMAO could capture water.

Unlike conventional AIMD simulations, EFP-MD can be utilized to investigate the time evolution of dipole moments in aqueous TMAO/TBA solutions (Figure 2). On average, the dipole moment of each water molecule is enhanced (4.20 D, +46%) when it approaches the N^+O^- group of TMAO. Similarly, when the water molecule approaches the OH group of TBA, the

dipole moment is enhanced (3.78 D, +32%). The ensemble averages indicate that water molecules near the N^+O^- group of TMAO (r < 3.5 Å) and the corresponding OH group of TBA increased the dipole moment by an average of 3.22 D (+12%) and 3.01 D (+5%), respectively, compared to the water molecules in pure water (Table S7). The former exhibits a more significant dipole moment because TMAO has a large dipole moment of 9.39 D in an aqueous solution. In general, molecules are stabilized by polarization in aggregated systems. Surprisingly, compared to the water molecules in pure water, the water molecules near the CH_3– group of TMAO and TBA were found to have a decreased dipole moment (by 1% and 3%, respectively; Table S7). This is because the steric barrier of the CH_3– group allows only a small number of water molecules to be coordinated around the waters with decreased dipole moments. The ensemble averages of the dipole moments indicate that the influence of the solute on water converges around 4.5 Å (Figure 3 and Table S7).

The enhancing and diminishing of polarization on the surrounding water are considered to appear as differences in the interaction energy components (E^{ES}, E^{EXREP}, E^{POL}, E^{CT}, and E^{DISP}) in the aqueous TMAO/TBA solution (Figures 4, S7, S8, and Tables S8, S9). Therefore, the interaction energy components near the hydrophilic/hydrophobic groups are discussed.

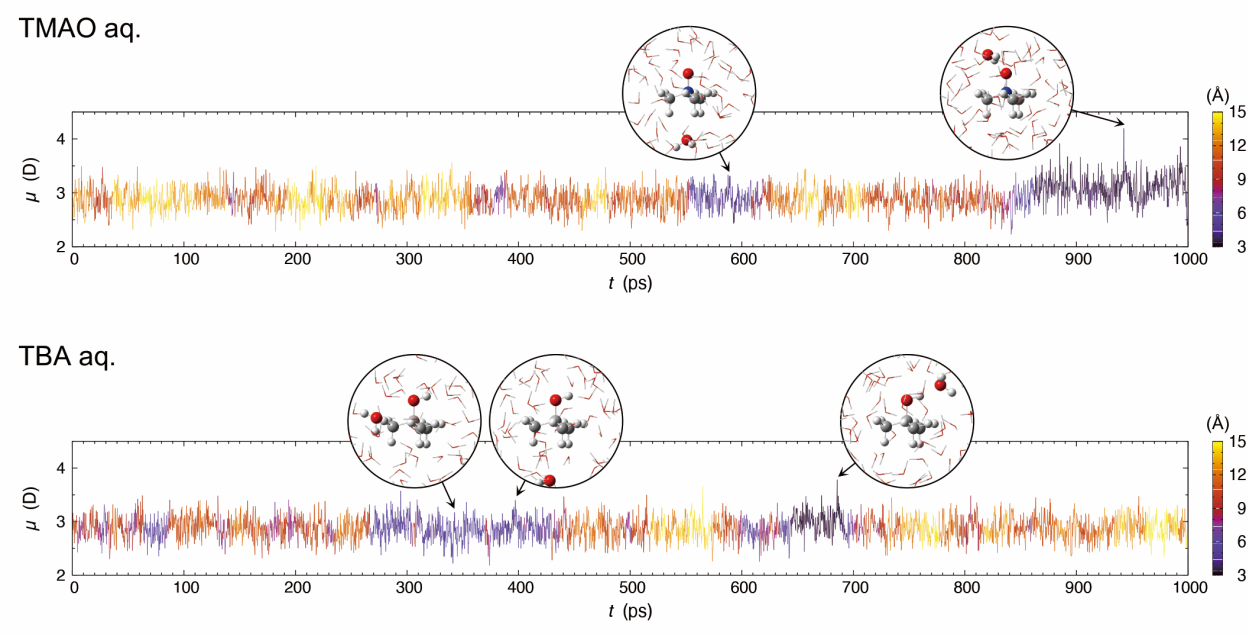

Figure 2. Temporal evolution of water dipole moments along 1 ns EFP-MD. The plot color represents the distances (NTMAO–Owater/CTBA–Owater) as indicated by the key on the right.

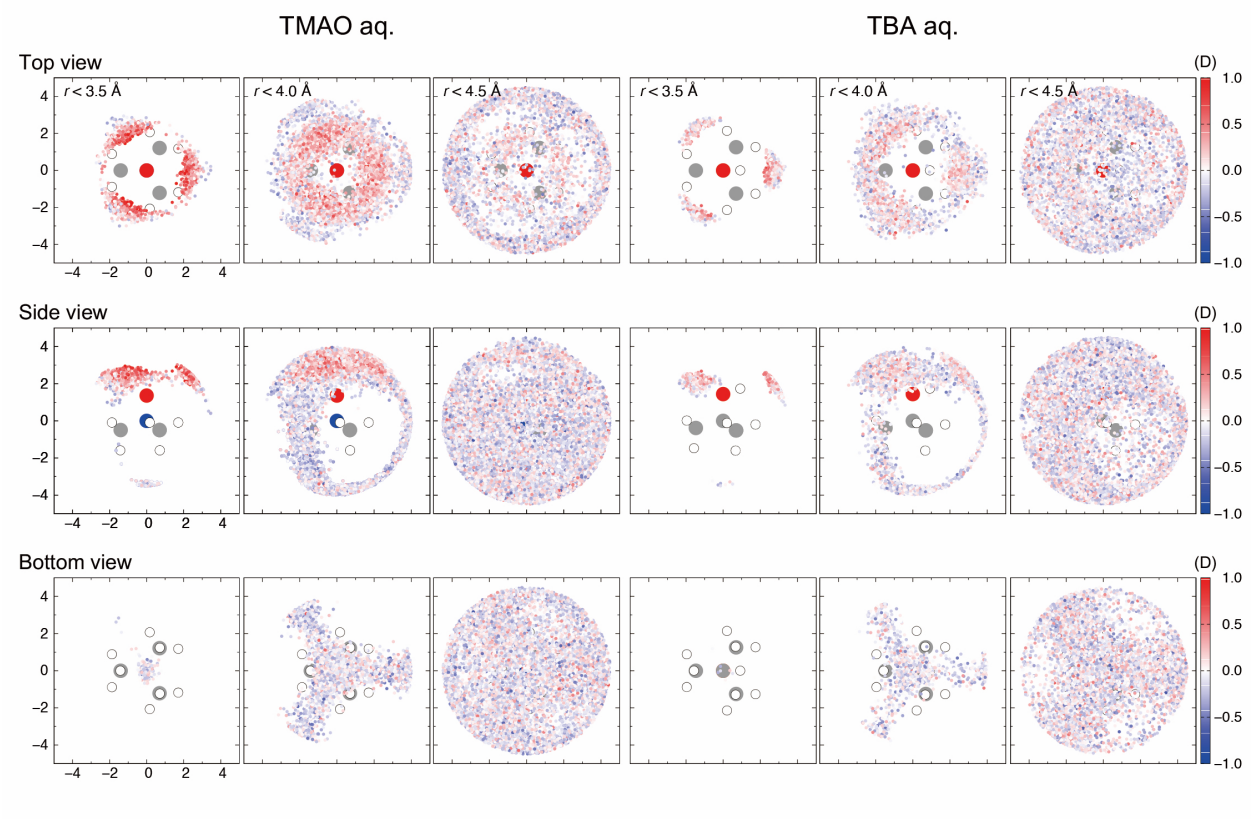

Figure 3. 1 ns water fluctuation colored by the dipole moments of H_2O molecules. The water molecules within 3.5, 4.0, and 5.0 Å from the solute are observed from the top, side, and bottom. The plot color represents the deviation from the pure water (2.87 D).

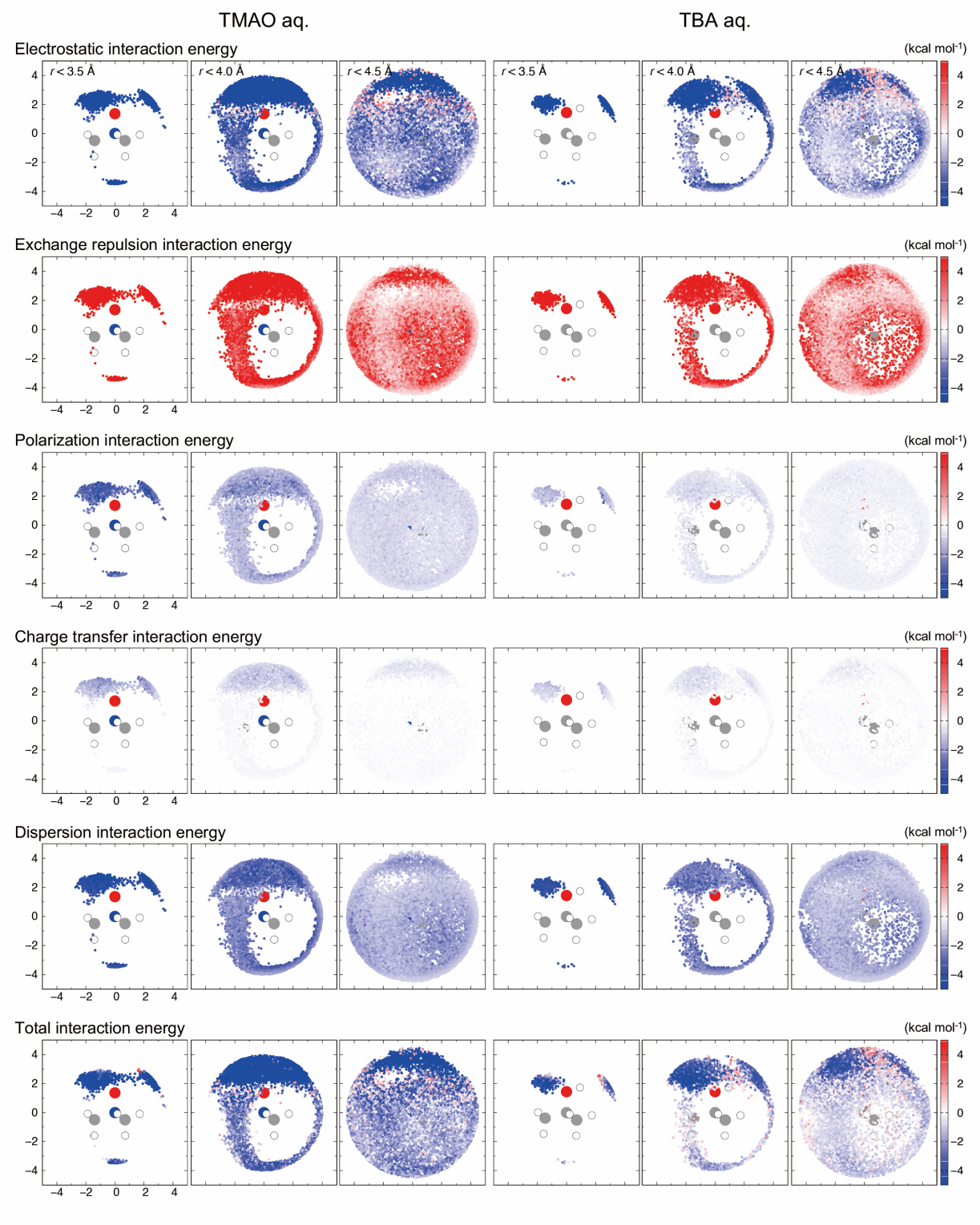

Figure 4. 1 ns water fluctuation colored by TMAO/TBA–water interactions. The water molecules within 3.5, 4.0, and 5.0 Å from the solute are observed from the side.

First, the solute–solvent polarization and charge-transfer interactions in the vicinity of the N^+O^- sites (r < 3.5 Å) in the TMAO solution were more than twice those corresponding to the OH sites in the TBA solution (Figures 4, S7, and Table S8). The natural bond orbital analysis explains the charge-transfer interaction with a dimer model (Figures S9, S10 and Table S10). The proton acceptor orbital of TMAO has a significant overlap integral with the H_2O orbital around the hydrophilic group and facilitates the charge-transfer (0.04 e). However, the orbital overlap between the OH groups of TBA and H_2O is small; thus, the charge-transfer is small (0.01 e). Therefore, we can conclude that the factors that cause the N^+O^- group to strongly supplement water in an aqueous TMAO solution are the polarization and charge-transfer interactions derived from the large polarization of TMAO.

Next, we analyzed the interaction between the CH_3– group and the surrounding water molecules (r < 3.5 Å) in a TMAO/TBA solution. In this instance, the difference in the solute does not cause any difference in the charge-transfer and dispersion interactions. This can be explained by the small overlap between the proton donor orbitals of the CH_3– groups of TMAO/TBA and the molecular orbitals of water (Figures S9, S10, Table S10). However, the polarization interaction energy of TMAO is more than twice that of TBA. The large dipole moment of TMAO in an aqueous solution affects even the CH_3– group. Assuming that the polarization interaction was zero, the interaction between the CH_3– group of TMAO and water would stabilize at –0.8 kcal mol^{-1} because of the contribution of the dispersion interaction, which is similar to that of TBA, and a hydrophobic interaction would be induced. In conclusion, the attractive interactions near the CH_3– group of TMAO are characterized by polarization interactions.

4. CONCLUSIONS

In conclusion, this study represents an unprecedented attempt to discuss the influence of an osmolyte TMAO and a denaturant TBA on the electronic state fluctuations of aqueous solutions by analyzing the time evolution of the intermolecular interactions; these interactions can be evaluated back to their physicochemical origin only via the *ab initio* EFP-MD method. The nanosecond-order EFP-MD method succeeded in reproducing the experimental diffusion coefficients. Our simulation results indicated that in dilute aqueous solutions, the dipole moment of the water molecules near the hydrophilic group of TMAO and TBA increased by an average of 12% and 5%, respectively. The dipole moment of the CH_3– group decreased by an average of 1% and 3% for TMAO and TBA, respectively. Surprisingly, when the chemical structures of the solutes were similar, the solute–solvent interaction characteristics changed depending on the local structure and polarity of the site. That is, TMAO allowed stable polarization and charge-transfer interactions with water molecules near the hydrophilic group, and the large solute polarization affected water molecules near the CH_3– group. However, the polarization of TBA was negligible and did not affect water molecules near the CH_3– group; the interaction was hydrophobic. The effect of small amphiphilic molecules on the change in the electronic state in aqueous solutions is significant, and it is important to investigate the mechanism by which osmolytes and denaturants control the stability of or denature proteins in biological environments. Our results indicate that we should take electronic fluctuation effects into account, for example in artificial chaperone design and anti-atherosclerosis drug development in next generation medicine.

REFERENCES

(1) Yancey, P. H.; Clark, M. E.; Hand, S. C.; Bowlus, R. D.; Somero, G. N. Living with Water Stress: Evolution of Osmolyte Systems. *Science* **1982**, *217*, 1214–1222, DOI:10.1126/science.7112124.

(2) Liao, Y. -T.; Manson, A. C.; DeLyser, M. R.; Noid, W. G.; Cremer, P. S. Trimethylamine N-oxide Stabilizes Proteins via a Distinct Mechanism Compared with Betaine and Glycine. *Proc. Natl. Acad. Sci. U.S.A.* **2017**, *114*, 2479–2484, DOI:10.1073/pnas.1614609114.

(3) Bennion, B. J.; Daggett, V. Counteraction of Urea-induced Protein Denaturation by Trimethylamine N-oxide: A Chemical Chaperone at Atomic Resolution. *Proc. Natl. Acad. Sci. U.S.A.* **2004**, *101*, 6433–6438, DOI:10.1073/pnas.0308633101.

(4) Canchi, D. R.; Jayasimha, P.; Rau, D. C.; Makhatadze, G. I.; Garcia, A. E. Molecular Mechanism for the Preferential Exclusion of TMAO from Protein Surfaces. *J. Phys. Chem. B* **2012**, *116*, 12095–12104, DOI:10.1021/jp304298c.

(5) Freda, M.; Onori, G.; Santucci, A. Infrared Study of the Hydrophobic Hydration and Hydrophobic Interactions in Aqueous Solutions of *tert*-Butyl Alcohol and Trimethylamine-N-oxide. *J. Phys. Chem. B* **2001**, *105*, 12714–12718, DOI:10.1021/jp011673m.

(6) Sinibaldi, R.; Casieri, C.; Melchionna, S.; Onori, G.; Segre, A. L.; Viel, S.; Mannina, L.; De Luca, F. The Role of Water Coordination in Binary Mixtures. A Study of Two Model Amphiphilic Molecules in Aqueous Solutions by Molecular Dynamics and NMR. *J. Phys. Chem. B* **2006**, *110*, 8885–8892, DOI:10.1021/jp056897+.

(7) Rezus, Y. L. A.; Bakker, H. J. Observation of Immobilized Water Molecules around Hydrophobic Groups. *Phys. Rev. Lett.* **2007**, *99*, 148301, DOI:10.1103/PhysRevLett.99.148301.

(8) Qvist, J.; Halle, B. Thermal Signature of Hydrophobic Hydration Dynamics. *J. Am. Chem. Soc.* **2008**, *130*, 10345–10353, DOI:10.1021/ja802668w.

(9) Panuszko, A.; Bruździak, P.; Zielkiewicz, J.; Wyrzykowski, D.; Stangret, J. Effects of Urea and Trimethylamine-N-oxide on the Properties of Water and the Secondary Structure of Hen Egg White Lysozyme. *J. Phys. Chem. B* **2009**, *113*, 14797–14809, DOI:10.1021/jp904001m.

(10) Bakulin, A. A.; Pshenichnikov, M. S.; Bakker, H. J.; Petersen, C. Hydrophobic Molecules Slow Down the Hydrogen-bond Dynamics of Water. *J. Phys. Chem. A* **2011**, *115*, 1821–1829, DOI:10.1021/jp107881j.

(11) Mazur, K.; Heisler, I. A.; Meech, S. R. THz Spectra and Dynamics of Aqueous Solutions Studied by the Ultrafast Optical Kerr Effect. *J. Phys. Chem. B* **2011**, *115*, 2563–2573, DOI:10.1021/jp111764p.

(12) Munroe, K. L.; Magers, D. H.; Hammer, N. I. Raman Spectroscopic Signatures of Noncovalent Interactions between Trimethylamine N-oxide (TMAO) and Water. *J. Phys. Chem. B* **2011**, *115*, 7699–7707, DOI:10.1021/jp203840w.

(13) Hunger, J.; Tielrooij, K.; Buchner, R.; Bonn, M.; Bakker, H. J. Complex Formation in Aqueous Trimethylamine-N-oxide (TMAO) Solutions. *J. Phys. Chem. B* **2012**, *116*, 4783–4795, DOI:10.1021/jp212542q.

(14) Ma, J.; Pazos, I. M.; Gai, F. Microscopic Insights into the Protein-stabilizing Effect of Trimethylamine N-oxide (TMAO). *Proc. Natl. Acad. Sci. U.S.A.* **2014**, *111*, 8476–8481, DOI:10.1073/pnas.1403224111.

(15) Usui, K.; Hunger, J.; Sulpizi, M.; Ohto, T.; Bonn, M.; Nagata, Y. *Ab Initio* Liquid Water Dynamics in Aqueous TMAO Solution. *J. Phys. Chem. B* **2015**, *119*, 10597–10606, DOI:10.1021/acs.jpcb.5b02579.

(16) Imoto, S.; Forbert, H.; Marx, D. Water Structure and Solvation of Osmolytes at High Hydrostatic Pressure: Pure Water and TMAO Solutions at 10 kbar Versus 1 bar. *Phys. Chem. Chem. Phys.* **2015**, *17*, 24224–24237, DOI:10.1039/C5CP03069B.

(17) Stirnemann, G.; Duboué-Dijon, E.; Laage, D. *Ab Initio* Simulations of Water Dynamics in Aqueous TMAO Solutions: Temperature and Concentration Effects. *J. Phys. Chem. B* **2017**, *121*, 11189–11197, DOI:10.1021/acs.jpcb.7b09989.

(18) Imoto, S.; Forbert, H.; Marx, D. Aqueous TMAO Solutions as Seen by Theoretical THz Spectroscopy: Hydrophilic Versus Hydrophobic Water. *Phys. Chem. Chem. Phys.* **2018**, *20*, 6146–6158, DOI:10.1039/C7CP07003A.

(19) Xie, W. J.; Cha, S.; Ohto, T.; Mizukami, W.; Mao, Y.; Wagner, M.; Bonn, M.; Hunger, J.; Nagata, Y. Large Hydrogen-bond Mismatch between TMAO and Urea Promotes Their Hydrophobic Association. *Chem.* **2018**, *4*, 2615–2627, DOI:10.1016/j.chempr.2018.08.020.

(20) Sahle, C. J.; Schroer, M. A.; Niskanen, J.; Elbers, M.; Jeffries, C. M.; Sternemann, C. Hydration in Aqueous Osmolyte Solutions: The Case of TMAO and Urea. *Phys. Chem. Chem. Phys.* **2020**, *22*, 11614–11624, DOI:10.1039/C9CP06785J.

(21) Mori, H.; Hirayama, N.; Komeiji, Y.; Mochizuki, Y. Differences in Hydration between *cis*- and *trans*-platin: Quantum Insights by *Ab Initio* Fragment Molecular Orbital-based Molecular Dynamics (FMO-MD). *Comput. Theor. Chem.* **2012**, *986*, 30–34, DOI:10.1016/j.comptc.2012.02.008.

(22) Matsuda, A.; Mori, H. Theoretical Study on the Hydration Structure of Divalent Radium Ion Using Fragment Molecular Orbital-Molecular Dynamics (FMO-MD) Simulation. *J. Solution Chem.* **2014**, *43*, 1669–1675, DOI:10.1007/s10953-014-0235-7.

(23) Kuroki, N.; Mori, H. Effective Fragment Potential Version 2 - Molecular Dynamics (EFP2-MD) Simulation for Investigating Solution Structures of Ionic Liquids. *Chem. Lett.* **2016**, *45*, 1009–1011, DOI:10.1246/cl.160366.

(24) Kuroki, N.; Mori, H. Applicability of Effective Fragment Potential Version 2 - Molecular Dynamics (EFP2-MD) Simulations for Predicting Excess Properties of Mixed Solvents. *Chem. Phys. Lett.* **2018**, *694*, 82–85, DOI:10.1016/j.cplett.2018.01.042.

(25) Kuroki, N.; Mori, H. Applicability of Effective Fragment Potential Version 2-Molecular Dynamics (EFP2-MD) Simulations for Predicting Dynamic Liquid Properties Including the Supercritical Fluid Phase. *J. Phys. Chem. B* **2019**, *123*, 194–200, DOI:10.1021/acs.jpcb.8b07446.

(26) Bandyopadhyay, D.; Kamble, Y.; Choudhury, N. How Different Are the Characteristics of Aqueous Solutions of *tert*-Butyl Alcohol and Trimethylamine-N-oxide? A Molecular Dynamics Simulation Study. *J. Phys. Chem. B* **2018**, *122*, 8220-8232, DOI:10.1021/acs.jpcb.8b02411.

(27) Gaussian 16, Revision C.01, Frisch, M. J.; Trucks, G. W.; Schlegel, H. B.; Scuseria, G. E.; Robb, M. A.; Cheeseman, J. R.; Scalmani, G.; Barone, V.; Petersson, G. A.; Nakatsuji, H.; Li, X.; Caricato, M.; Marenich, A. V.; Bloino, J.; Janesko, B. G.; Gomperts, R.; Mennucci, B.; Hratchian, H. P.; Ortiz, J. V.; Izmaylov, A. F.; Sonnenberg, J. L.; Williams-Young, D.; Ding, F.; Lipparini, F.; Egidi, F.; Goings, J.; Peng, B.; Petrone, A.; Henderson, T.; Ranasinghe, D.; Zakrzewski, V. G.; Gao, J.; Rega, N.; Zheng, G.; Liang, W.; Hada, M.; Ehara, M.; Toyota, K.; Fukuda, R.; Hasegawa, J.; Ishida, M.; Nakajima, T.; Honda, Y.; Kitao, O.; Nakai, H.; Vreven, T.; Throssell, K.; Montgomery Jr., J. A.; Peralta, J. E.; Ogliaro, F.; Bearpark, M. J.; Heyd, J. J.; Brothers, E. N.; Kudin, K. N.; Staroverov, V. N.; Keith, T. A.; Kobayashi, R.; Normand, J.; Raghavachari, K.; Rendell, A. P.; Burant, J. C.; Iyengar, S. S.; Tomasi, J.; Cossi, M.; Millam, J. M.; Klene, M.; Adamo, C.; Cammi, R.; Ochterski, J. W.; Martin, R. L.; Morokuma, K.; Farkas, O.; Foresman, J. B.; Fox, D. J. Gaussian, Inc., Wallingford CT, 2019.

(28) Dunning Jr., T. H. Gaussian Basis Sets for Use in Correlated Molecular Calculations. I. The Atoms Boron through Neon and Hydrogen. *J. Chem. Phys.* **1989**, *90*, 1007–1023, DOI:10.1063/1.456153.

(29) Lee, T. J.; Taylor, P. R. A Diagnostic for Determining the Quality of Single-reference Electron Correlation Methods. *Int. J. Quant. Chem.* **1989**, *36*, 199–207, DOI:10.1002/qua.560360824.

(30) Schmidt, M. W.; Baldridge, K. K.; Boatz, J. A.; Elbert, S. T.; Gordon, M. S.; Jensen, J. H.; Koseki, S.; Matsunaga, N.; Nguyen, K. A.; Su, S.; Windus, T. L.; Dupuis, M.; Montgomery,

J. A. General Atomic and Molecular Electronic Structure System, *J. Comput. Chem.* **1993**, *14*, 1347–1363, DOI:10.1002/jcc.540141112.

(31) Su, P.; Li, H. Energy Decomposition Analysis of Covalent Bonds and Intermolecular Interactions. *J. Chem. Phys.* **2009**, *131*, 014102, DOI:10.1063/1.3159673.

(32) Markthaler, D.; Zeman, J.; Baz, J.; Smiatek, J.; Hansen, N. Validation of Trimethylamine-N-oxide (TMAO) Force Fields Based on Thermophysical Properties of Aqueous TMAO Solutions. *J. Phys. Chem. B* **2017**, *121*, 10674–10688, DOI:10.1021/acs.jpcb.7b07774.

(33) Harris, K. R.; Woolf, L. A. Pressure and Temperature Dependence of the Self Diffusion Coefficient of Water and Oxygen-18 Water. *J. Chem. Soc., Faraday Trans. 1* **1980**, *76*, 377–385, DOI:10.1039/F19807600377.

(34) Clark, M. E.; Burnell, E. E.; Chapman, N. R.; Hinke, J. A. Water in Barnacle Muscle. IV. Factors Contributing to Reduced Self-diffusion. *Biophys. J.* **1982**, *39*, 289–299, DOI:10.1016/S0006-3495(82)84519-0.

(35) Paul, S.; Patey, G. N. Why *tert*-Butyl Alcohol Associates in Aqueous Solution But Trimethylamine-N-oxide Does Not. *J. Phys. Chem. B* **2006**, *110*, 10514–10518, DOI:10.1021/jp0609378.

(36) Luzar, A.; Chandler, D. Hydrogen-bond Kinetics in Liquid Water. *Nature* **1996**, *379*, 55–57, DOI:10.1038/379055a0.